Medical Physics
The International Journal of Medical Physics Research and Practice

Commissioning the neutron production of a Linac: Development of a simple tool for second cancer risk estimation

M. Romero-Expósito, B. Sánchez-Nieto, J. A. Terrón, M. C. Lopes, B. C. Ferreira, D. Grishchuk, C. Sandín, S. Moral-Sánchez, M. Melchor, C. Domingo, F. Gómez, and F. Sánchez-Doblado

Citation: Medical Physics **42**, 276 (2015); doi: 10.1118/1.4903525
View online: http://dx.doi.org/10.1118/1.4903525
View Table of Contents: http://scitation.aip.org/content/aapm/journal/medphys/42/1?ver=pdfcov
Published by the American Association of Physicists in Medicine

Commissioning the neutron production of a Linac: Development of a simple tool for second cancer risk estimation

M. Romero-Expósito[a)]
Departamento de Fisiología Médica y Biofísica, Universidad de Sevilla, Sevilla 41009, Spain and Departament de Física, Universitat Autònoma de Barcelona, Bellaterra 08193, Spain

B. Sánchez-Nieto
Instituto de Física, Pontificia Universidad Católica de Chile, Santiago 4880, Chile

J. A. Terrón
Servicio de Radiofísica, Hospital Universitario Virgen Macarena, Sevilla 41009, Spain

M. C. Lopes
Serviço de Física Médica, Instituto Português de Oncologia, Coimbra 3000-075, Portugal

B. C. Ferreira
i3N, Department of Physics, University of Aveiro, Aveiro 3810-193, Portugal

D. Grishchuk
Radiotherapy Service, Russian Research Center for Radiology and Surgical Technology, Saint Petersburg 197758, Russian Federation

C. Sandín
Elekta, Ltd., Crawley RH10 9RR, United Kingdom

S. Moral-Sánchez
Servicio de Radiofísica, Instituto Onkologikoa, San Sebastián 20014, Spain

M. Melchor
Servicio de Radiofísica, Hospital Universitario de la Ribera, Alzira 46600, Valencia, Spain

C. Domingo
Departament de Física, Universitat Autònoma de Barcelona, Bellaterra 08193, Spain

F. Gómez
Departamento de Física de Partículas, Universidad de Santiago de Compostela, Santiago de Compostela 15782, Spain

F. Sánchez-Doblado
Departamento de Fisiología Médica y Biofísica, Universidad de Sevilla, Sevilla 41009, Spain and Servicio de Radiofísica, Hospital Universitario Virgen Macarena, Sevilla 41009, Spain

(Received 22 January 2014; revised 20 November 2014; accepted for publication 23 November 2014; published 23 December 2014)

Purpose: Knowing the contribution of neutron to collateral effects in treatments is both a complex and a mandatory task. This work aims to present an operative procedure for neutron estimates in any facility using a neutron digital detector.
Methods: The authors' previous work established a linear relationship between the total second cancer risk due to neutrons (TR^n) and the number of MU of the treatment. Given that the digital detector also presents linearity with MU, its response can be used to determine the TR^n per unit MU, denoted as m, normally associated to a generic Linac model and radiotherapy facility. Thus, from the number of MU of each patient treatment, the associated risk can be estimated. The feasibility of the procedure was tested by applying it in eight facilities; patients were evaluated as well.
Results: From the reading of the detector under selected irradiation conditions, m values were obtained for different machines, ranging from 0.25×10^{-4}% per MU for an Elekta Axesse at 10 MV to 6.5×10^{-4}% per MU for a Varian Clinac at 18 MV. Using these values, TR^n of patients was estimated in each facility and compared to that from the individual evaluation. Differences were within the range of uncertainty of the authors' methodology of equivalent dose and risk estimations.
Conclusions: The procedure presented here allows an easy estimation of the second cancer risk due to neutrons for any patient, given the number of MU of the treatment. It will enable the consideration of this information when selecting the optimal treatment for a patient by its implementation in the treatment planning system. [http://dx.doi.org/10.1118/1.4903525]

Key words: peripheral dose, neutrons, second cancer risk, TPS algorithm

1. INTRODUCTION

Photoneutrons are produced in linear accelerators at high energy operation mode (i.e., above 8 MV) as a result of photonuclear interactions in shielding material.[1] Consequently, patients are also exposed to neutrons during their photon radiotherapy (RT) treatment. The main problem is neutrons' high relative biological effectiveness (RBE). For the same absorbed dose, neutrons at about 1 MeV, which is the energy range typically exhibited by fast neutrons produced in RT rooms,[2] can be 20 times more damaging than photons.[3]

However, determining neutron doses received by patients is not an easy task. The energy dependence of RBE makes essential to determine the energy spectra of neutrons. In addition to this previous difficulty, under RT conditions (pulsed and mixed γ-n fields), only passive detectors, which require considerable time for processing, analysis, and evaluation, have traditionally been recommended.[4] Thus, neutron doses are not usually evaluated, and consequently ignored, during patient treatment.

Different approaches have been used for neutron fluence and equivalent dose determination in specific treatments, generally of prostate.[5–8] A new methodology, introduced in Sánchez-Doblado *et al.*,[9] allows to estimate neutron equivalent dose in organs in real time, for patients under any RT treatment, from the readings of a neutron digital detector.[10] This detector takes measurements during the irradiation of the treatment, and thereafter, its reading is translated to an equivalent dose through some organ-specific coefficients. Thanks to the easy implementation, it was used to carry out a clinical study to estimate the neutron equivalent dose for more than 1000 patients in 42 different facilities and for several pathologies.[11] This methodology estimates the equivalent organ dose together with the nominal risk of acquiring a second cancer in each organ and, from them, the total risk due to neutrons (TR^n). Estimates were based on the risk model taken from ICRP-103.[3] One important result was the linear dependence of neutron doses and risks on MU.[11] The linear relationships between TR^n and MU were modeled for 15 different combinations of Linac energy and manufacturer. The former allows a quick estimation of TR^n whenever the digital detector is not available.

Although there is a strong linear correlation between TR^n and MU for the different Linac models, some exceptions were found. In particular, for the Varian Clinac 18 MV, a deeper analysis of data seemed to suggest that, regarding neutron production, two of the accelerators of the same model gave significantly different results.[11] That is, the "same Linac model" would not necessarily imply the "same behavior in terms of neutron production" in the actual facility. There may be little modifications in Linac design, with no consequences to photon beams, but with significant differences in neutron production.

Therefore, this work aims to propose another alternative option to the use of the reference values of TR^n per MU. This involves a simple experimental procedure (a single measurement using the digital detector under established conditions) to characterize the neutron production of a specific Linac. This option could provide a more accurate relationship between TR^n and MU than the reference model and has to be carried out just once (as the data generated during the commissioning stage). After describing the procedure, and to test its feasibility, the results of the comparison of the TR^n estimations from this characterization model, with the results obtained using the digital detector during each treatment, are presented for 220 patients irradiated in 8 Linacs in 5 different facilities. A comparison of individual Linac characterization and reference models is also provided.

2. METHOD AND MATERIAL

2.A. Neutron digital detector

The digital detector is based on the sensitivity of static random access memory (SRAM) devices to thermal neutron fluence.[12] Single event upsets (SEU) of memory states are produced in the detector because of the interactions, so they are proportional to the neutron thermal fluence reaching the detector.[10,13] A thorough description of the detector can be found in Gómez *et al.*[10] During irradiation, the detector in the RT room must be placed in front of the rotation gantry axis and close to the wall.[14]

2.B. Second cancer estimation

According to Expósito *et al.*,[11] TR^n can be obtained from the following expression:

$$TR^n = \left(\sum_i \mathrm{DDREF} \cdot \lambda_i^k \cdot g_{i,j} \right) \cdot \frac{\mathrm{DD}}{F_A}, \quad (1)$$

where DDREF is the dose and dose-rate effectiveness factor; λ_i^k, the incidence risk coefficients per organ i and gender k; $g_{i,j}$, the equivalent-dose-per-event factor in the organ i for treatment j;[9] DD, the digital detector reading; and F_A, the bunker-size correction factor.[9] The latter takes into account the effect of the size of the bunker on the thermal distribution of neutrons.

In order to simplify the notation, the summation between brackets will be noted as the *Events-to-Risk Factor* ($\mathrm{ERF}_{k,j}$). Incidence risk coefficients and DDREF can be obtained from reports on the effects of radiation and the induction of cancer.[3,15] In this work, we selected ICRP Publication 103 to obtain the risk coefficients λ_i [Table A.4.1 in ICRP-103 (Ref. 3)] and the value of DDREF (=2). The summation will extend to a different number of organs depending on the gender. For example, in females, breast and ovaries must be added to the considered organs in males (esophagus, stomach, colon, liver, lung, bladder, thyroid, bone surface, red marrow, skin, and the remainder). The $g_{i,j}$ coefficients were previously calculated for two general types of treatments: head and neck treatments and treatments at the rest of the body (referred to as abdomen treatments[9,11]). Thus, the $\mathrm{ERF}_{k,j}$ depends on the gender and type of treatment and, in consequence, there are four different values given by the different combinations of both parameters. These values are: 5.8×10^{-5}% for male head,

6.3×10^{-5}% for male abdomen, 6.0×10^{-5}% for female head, and 6.7×10^{-5}% for female abdomen. Given the difficulties in assigning uncertainties to risk coefficients or even DDREF, we estimated the uncertainty of these $ERF_{k,j}$ only from the uncertainty of the $g_{i,j}$ coefficients, that is, around 30%.[9]

The approach for risk calculation using Eq. (1) necessarily requires the use of the digital detector during the treatment of the patient. Alternatively, given that a linear association was found between TR^n and MU,[11] TR^n can be also estimated as follows:

$$TR^n = m \cdot MU, \tag{2}$$

where m (in risk per MU) depends on the Linac model (manufacturer and energy). In Expósito *et al.*,[11] general values of m were tabulated for 15 different Linac models, that is, they can be used for every patient. However, this equation can also be formulated as a function of gender and type of treatment, a specification not performed in our previous work owing to statistical reasons (small groups).

Therefore, Eqs. (1) or (2) can alternatively be used for the estimation of the TR^n but with a different level of uncertainty (see Sec. 4).

2.C. Facility characterization

Our proposal is based on the fact that, given that the digital detector is sensitive to thermal neutrons, which in turn are proportional to the global production of neutrons, the number of events in the detector is also proportional to the number of MU (Ref. 10) and can be written as

$$DD = c \cdot MU. \tag{3}$$

Substituting Eq. (3) into Eq. (1) and then comparing with Eq. (2), m is given by

$$m_{k,j} = ERF_{k,j} \cdot \frac{c}{F_A}. \tag{4}$$

In our previous experiments, the events in the digital detector showed no significant dependence on field size or treatment type.[9] Then, for practical reasons, the usual reference irradiation conditions (gantry angle at 0° and field size of 10×10 cm^2) were chosen to measure the number of events associated to a certain number of MU.

If DD_{1000} denotes the mean number of events obtained with 1000 MU at the digital detector under these irradiation conditions, c can be calculated from Eq. (3) and substituting into Eq. (4) gives

$$m_{k,j} = ERF_{k,j} \cdot \frac{DD_{1000}}{F_A \cdot 1000}. \tag{5}$$

The c factor (in events per MU) accounts for the neutron production rate of a specific Linac and was estimated for the eight different facilities in the five centers described in Table I. After this characterization, TR^n can be estimated from the MU through the $m_{k,j}$ parameter, which is specific to the Linac model, patient gender, and type of treatment.

2.D. Patients

After the characterization of the eight installations, TR^n values were estimated for 220 patients from the same centers using the characterization model [that is, Eq. (2) with the calculated $m_{k,j}$ value], the reference model [Eq. (2) with the m value of the corresponding Linac from Expósito *et al.*[11]—noted as $m_{\text{ref. model}}$], and the reading of the digital detector during the irradiation of each patient [Eq. (1)]. Measurements were carried out during a normal workday in each facility; no specific treatments were selected. In particular, for this subset of patients from the cohort of Expósito *et al.*,[11] prostate was the most common treatment (38% of cases), followed by rectum, breast, and head and neck (13%, 13%, and 10%, respectively). Only 10% of the treatments were delivered by IMRT. The breast and head and neck treatments used both high and low energy beams.

3. RESULTS

Equations (3) and (5) were used for the determination of the c and $m_{k,j}$ values in the eight facilities in Table I. For the sake of simplicity in presenting the results, an averaged value of $ERF_{k,j}$ ($ERF_{\text{mean}} = 62\times10^{-6}$%) will be used for calculations. This is a good approximation as the high value of the risk

TABLE I. Facility characteristics.

Facility	Linac	Nominal energy (MV)	Bunker room surface (m^2)	F_A[a]
MI[b]	Elekta Axesse	10, 15	70.31	0.927 ± 0.031
RRCRST[c]	Elekta Axesse	18	74.82	0.895 ± 0.031
IPO[d]	(1) Siemens Oncor	15	64.60	0.973 ± 0.031
	(2) Siemens Oncor	15	50.25	1.138 ± 0.035
Onkologikoa	(1) Varian Clinac 2100 C/D	18	51.84	1.116 ± 0.034
	(2) Varian Clinac 21 EX	18	51.84	1.116 ± 0.034
HR[e]	(1) Varian Clinac 2100 C	18	44.49	1.234 ± 0.037
	(2) Varian Clinac 2100 C/D	18	63.73	0.981 ± 0.032

[a]Values using equation in Sánchez-Doblado *et al.* (Ref. 9).
[b]Meshalkin Institute (Novosibirsk, Russia).
[c]Russian Research Center for Radiology and Surgical Technology (Saint Petersburg, Russia).
[d]Instituto Português de Oncologia (Coimbra, Portugal).
[e]Hospital de la Ribera (Alzira, Spain).

coefficient for skin, which is the same in all cases, dominates the calculations and it does not represent any change in the conclusions of the work. Nevertheless, a more accurate estimation would imply the use of the specific $ERF_{k,j}$ value.

Table II shows the c and the mean value of $m_{k,j}$ (m_{mean}), obtained using ERF_{mean}, for each installation. Uncertainties have been obtained from propagation, on average of the order of 4% and 30%, respectively. It has to be taken into account that the 30% has been obtained without assigning uncertainties to the risk coefficients and the DDREF. The corresponding slopes of the reference models ($m_{ref.\ model}$) have also been tabulated.

Figure 1 depicts, for the 220 patients grouped according to the facility, the TR^n values estimated from the measurements with the digital detector during the irradiation of each patient (symbols) and prediction with the characterization model (lines) using the corresponding m_{mean} value tabulated in Table II. Despite using the ERF_{mean}, experimental values are closely distributed around the predicted linear correlation.

A measure of the differences using the percentage RMS error between the risks predicted by both models (characterization and reference) and the values estimated using the digital detector during patient irradiation can be also found in Table II. The characterization of the specific machine allows a better estimation of the risk than using the general values reported in Expósito *et al.*[11]

4. DISCUSSION

The advantage of using the digital detector during patient irradiation is that it provides a simple and reliable measuring device whose readout can be used in conjunction with the model in Sánchez-Doblado *et al.*[9] The information so obtained could be used for retrospective studies, but neutron collateral effects could not be considered prospectively during the treatment planning process. By contrast, the use of the reference models in Expósito *et al.*,[11] which do not take into account the neutron production of a specific Linac, allows the estimation of the risks before applying the treatment, so that they can be considered as another treatment optimization parameter. Furthermore, in the case of a new model of Linac not included in Expósito *et al.*,[11] there is no reference model at all.

The methodology proposed here represents an alternative to the use of the reference models. The initial measurement with the digital detector allows the characterization of the neutron production at the specific installation, with the associated advantages of *a priori* estimation of TR^n (for example, allowing the comparison of two different plans to check which is better in terms of neutrons). Qualitatively, the characterization models behave well as can be seen in Fig. 1. TR^n estimations using the characterization presented a maximum relative deviation of 15% from the expected value. This deviation lays inside the relative uncertainty interval associated to our methodology around 30%.

As the characterization of neutron production consists, basically, in the determination of the steepness of the linear relationship between the risk and the MU for each specific Linac, the slopes for the characterization and reference models are very similar (Table II). As expected, RMS errors for the characterization model were also similar to the ones for the reference model but there are important exceptions. For example, there are two Varian Clinac 2100 for which the reference model over- and underestimates the risks by 29% approximately. This example illustrates and quantifies one of the benefits of carrying out the initial characterization.

It should be taken into account that we measure thermal neutron fluences inside the bunker, and these fluences are dependent on room volume. For this reason, we introduced F_A in our methodology. The equation modeling the behavior of thermal fluence with room size[9] allows correcting the reading of the detector in a way that we can compare Linacs as if they were installed in the same room. Therefore, readout differences would be due to differences between machines, and similar values should be obtained for machines of the same model. However, after carrying out the F_A correction, we still have differences in some c values of *a priori* equal Linacs. First, it should be noticed that equal machines are optimized in order to fulfill the same requirements only in terms of photon beam. Thus, the particular neutron production of a specific machine may not agree with the average of the model. This effect justifies the process of characterization.

TABLE II. m_{mean} calculated for each installation and steepness of the reference models ($m_{ref.\ model}$) [Expósito *et al.* (Ref. 13)] corresponding to each Linac. Percentage root mean square (RMS) error has been used to measure differences between risks estimated from individual measurements and the characterization and reference models.

Facility	Linac	Nominal energy (MV)	c (events per MU)	m_{mean} ($\times 10^{-4}$% per MU)	RMS_{charac}	$m_{ref.\ model}$ ($\times 10^{-4}$% per MU)[a]	$RMS_{ref.\ model}$
MI	Elekta Axesse	10	0.402 ± 0.064	0.249 ± 0.076	7.6	0.28	14
		15	1.276 ± 0.057	0.79 ± 0.24	5.7	0.83	12
RRCRST	Elekta Axesse	18	1.973 ± 0.082	1.22 ± 0.37	6.6	1.24	7
IPO	(1) Siemens Oncor	15	1.200 ± 0.053	0.74 ± 0.23	10	0.73	9.5
	(2) Siemens Oncor	15	1.446 ± 0.057	0.90 ± 0.27	15	0.73	21
Onkologikoa	(1) Varian Clinac 2100 C/D	18	7.28 ± 0.24	4.5 ± 1.4	7.2	4.74	10
	(2) Varian Clinac 21 EX	18	7.09 ± 0.23	4.4 ± 1.3	11	4.74	11
HR	(1) Varian Clinac 2100 C	18	10.43 ± 0.32	6.5 ± 2.0	14	4.74	29
	(2) Varian Clinac 2100 C/D	18	6.51 ± 0.23	4.0 ± 1.2	11	4.74	28

[a]Values from Expósito *et al.* (Ref. 13).

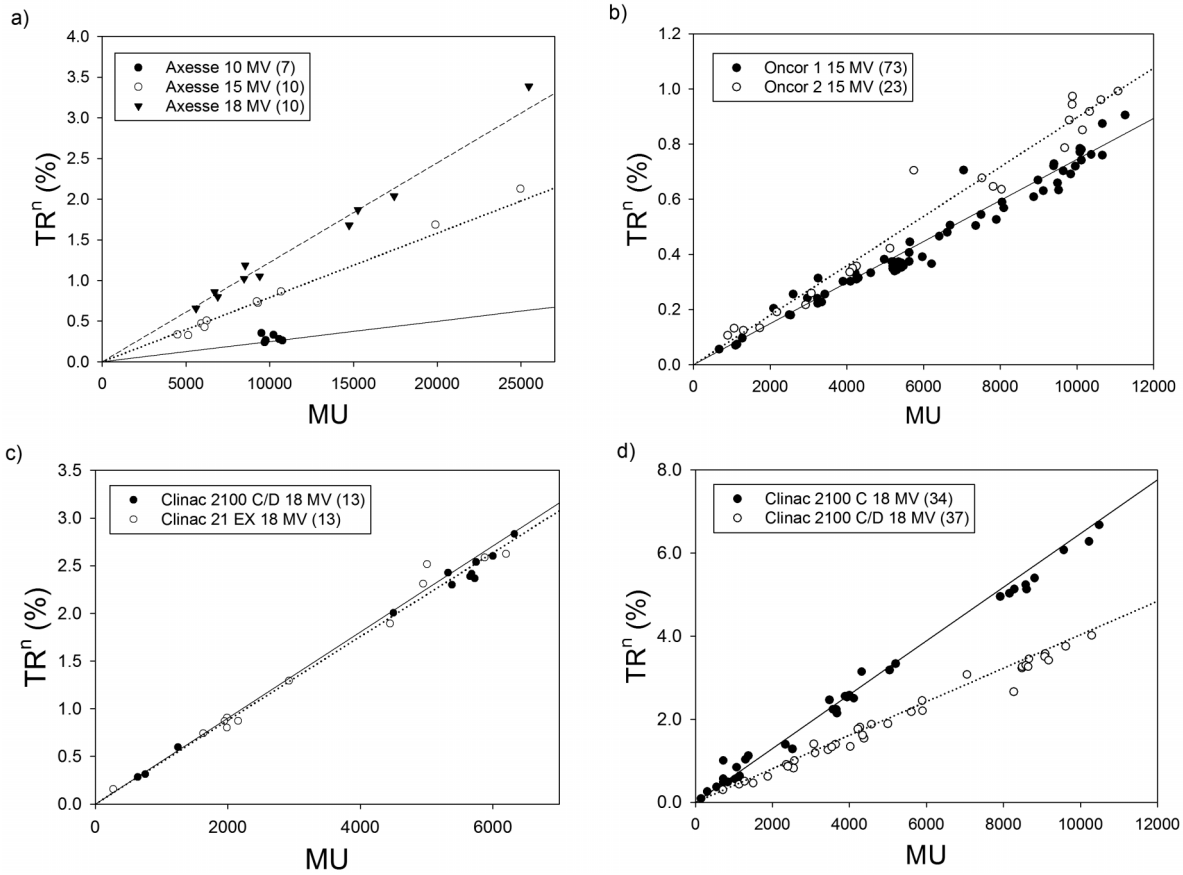

FIG. 1. TR^n of patients obtained from Eq. (1) using the measurements of the digital detector obtained during patient irradiation (symbols) together with the relation between TR^n and MU obtained using the proposed methodology (solid lines) in MI and RRCRST (a), IPO (b), Onkologikoa (c), and HR (d). Numbers in brackets in the legends represent the number of patients.

Additionally, F_A was obtained from Monte Carlo simulation of the thermal fluence in the detector location using a specific Linac in different bunkers, changing only the floor room area. Then, other geometric differences in bunker design, which could induce deviations in detector reading, are not considered in our correction. In any case, the m_{mean} values obtained for similar machines fit within the uncertainties.

Our benchmarks are the neutron equivalent dose in organs, estimated from the number of events in the detector during patient irradiation (explained in Sánchez-Doblado *et al.*[9]), with an uncertainty of approximately 30%. This uncertainty comes from the generalization of the $g_{i,j}$ coefficients for any Linac model and energy. Our first approach focused on neutrons arriving to the patient. However, other parameters, such as patient geometry and treatment dependence, had to be simplified due to the complexity of the experimental evaluation of doses. On one hand, the coefficients were obtained from in-phantom measurements so they applied for a "standard" man/woman, with no consideration of height or girth. On the other hand, just two general treatments were defined: for head and neck locations and for the rest of the body. Given that equivalent doses are mainly due to the fast neutrons coming directly from the Linac head, moderate changes in the location and size of the planning treatment volume will lead to small changes in the associated neutron dose. For example, all treatments in the pelvis region will lead to the same range of doses, at least, within the level of uncertainty of our methodology.

In Expósito *et al.*,[11] neutron equivalent doses in some organs for a prostate treatment were compared with results from other experimental works, showing congruent values with those previously published. This pointed that our methodology leads to acceptable risk estimations. Although comparisons with epidemiological papers have to be done with caution (for example, they cannot distinguish between the second cancers attributable to neutrons and the ones caused by photons and differences in machines and treatment strategies), the range of our estimations are similar to the incidences reported, for example, by Bartkowiak *et al.*[16] (4%) and Berrington *et al.*[17] (8%).

On the other hand, several publications have made risk estimations from evaluated doses for particular organs in specific treatments. It has to be taken into account that these estimations are dependent on the report used to extract risk coefficients. In our work, we used the ICRP, however, BEIR-VII (Ref. 15) has been used more commonly for risk estimations.[18,19] For example, Bednarz *et al.*,[18] reported, for a prostate treatment delivered with an 18 MV Varian Clinac to a 60 yr-old patient, a total lifetime attributable risk (for both photons and neutrons) of 8.3×10^{-5}% per MU. For similar machines characterized in our work, this risk increases up to around 5×10^{-4}% per MU, just for neutrons. This difference

can be explained by one of the most important differences between ICRP and BEIR reports, that is, the former assigns a high risk coefficient for skin (one order of magnitude over the rest), while the latter does not consider it. If we use the c value of one of the 18 MV Varian Linacs and recalculate the ERF using BEIR coefficients for a male patient of 60 yr, we obtain a risk of 5.5×10^{-5}% per MU. Assuming that photon risk has the same order of magnitude, our method yields similar risk values.

Note that our main efforts are directed to increasing the accuracy of the neutron equivalent dose in organs. However, in the case of risk estimations, it has to be borne in mind that it is not an easy task to evaluate the uncertainties; in fact, ICRP does not offer uncertainty for the risk coefficients. Therefore, the risk estimations presented will have higher uncertainties than 30% of our methodology. All work focused on establishing accurate neutron dosimetry will make it possible to develop accurate response models.

The measurement of the DD_{1000} using the digital detector could be included in the commissioning of the Linac, as any other parameter included in the Linac commissioning (for example, the PDD curves), and the equations, introduced in the treatment planning system (TPS). Thus, the second cancer risk associated to neutrons can be easily taken into account during the planning process and finally stored together with the dosimetric data in the patient medical report. A script for Pinnacle^3 (Philips) has been developed in collaboration with the Radiotherapy Service of University General Hospital of Valencia (Spain) for TR^n estimation, and it is being used in three hospitals in Spain. Nonetheless, if the TPS does not allow the use of scripts, the simplicity of the algorithm makes possible using it as an additional spread-sheet software.

It is worth noting that although our model has been built with our digital detector, the same methodology would be applicable to any other thermal-neutron-sensitive detector. A correction factor for the response of another appropriate neutron detector could be obtained following a cross-calibration procedure[20] and then, included into the expressions.

As a final comment, the total risk estimation from treatment MU could be a very useful tool for an integral radiobiological treatment evaluation, including not only tumor control probability (TCP) and normal tissue complication probability (NTCP), but also the second cancer risk due to out-of-field neutrons and photons.[21]

5. CONCLUSION

Given the linearity of doses and risks with MU, the characterization of any specific RT facility with a simple reference measurement seems a natural option. A single measurement using an accessible digital detector is the only requirement for this neutron production characterization. Therefore, the procedure presented here allows an easy estimation of the secondary cancer risk due to the neutron component from the number of MU, for any patient. Given that this information is obtained during the planning process, it can be used as another optimization parameter.

ACKNOWLEDGMENTS

The authors are indebted to the Spanish Nuclear Security Council (CSN) for its support through a specific agreement with the University of Seville for measuring neutron doses in radiotherapy patients. The experimental measurements would have been impossible without the kind collaboration of the radiophysicists and technicians in the different hospitals. The authors would also like to thank H. Galán-Dorado for her revision of grammar and style.

[a]Author to whom correspondence should be addressed. Electronic mail: mariateresa.romero@uab.cat

[1]NCRP, "Neutron contamination from medical accelerators," NCRP Report 79 (National Council on Radiation Protection and Measurements, Bethesda, 1984).
[2]J. Pena *et al.*, "Monte Carlo study of Siemens PRIMUS photoneutron production," Phys. Med. Biol. **50**, 5921–5933 (2005).
[3]ICRP, *The 2007 Recommendations of the International Commission on Radiological Protection (ICRP Publication 103)* (Elsevier, Amsterdam, 2007).
[4]AAPM, "Neutron measurements around high energy x-ray radiotherapy machines," AAPM Report 19 (Medical Physics Publishing, New York, NY, 1986).
[5]B. Bednarz, C. Hancox, and X. G. Xu, "Calculated organ doses from selected prostate treatment plans using Monte Carlo simulations and an anatomically realistic computational phantom," Phys. Med. Biol. **54**, 5271–5286 (2009).
[6]R. M. Howell *et al.*, "Calculation of effective dose from measurements of secondary neutron spectra and scattered photon dose from dynamic MLC IMRT for 6 MV, 15 MV, and 18 MV beam energies," Med. Phys. **33**, 360–368 (2006).
[7]S. F. Kry *et al.*, "Monte Carlo study shows no significant difference in second cancer risk between 6 and 18 MV intensity-modulated radiation therapy," Radiother. Oncol. **91**, 132–137 (2009).
[8]D. Verellen and F. Vanhavere, "Risk assessment of radiation-induced malignancies based on whole-body equivalent dose estimates for IMRT treatment in the head and neck region," Radiother. Oncol. **53**, 199–203 (1999).
[9]F. Sànchez-Doblado *et al.*, "Estimation of neutron-equivalent dose in organs of patients undergoing radiotherapy by the use of a novel online digital detector," Phys. Med. Biol. **57**, 6167–6191 (2012).
[10]F. Gómez, A. Iglesias, and F. Sánchez-Doblado, "A new active method for the measurement of slow-neutron fluence in modern radiotherapy treatment rooms," Phys. Med. Biol. **55**, 1025–1039 (2010).
[11]M. R. Expósito *et al.*, "Neutron contamination in radiotherapy: Estimation of second cancers based on measurements in 1377 patients," Radiother. Oncol. **107**, 234–241 (2013).
[12]R. Baumann and E. Smith, "Neutron-induced B-10 fission as a major source of soft errors in high density SRAMs," Microelectron. Reliab. **41**, 211–218 (2001).
[13]C. Domingo *et al.*, "Calibration of a neutron detector based on single event upset of SRAM memories," Radiat. Meas. **45**, 1513–1517 (2010).
[14]E. Jiménez-Ortega *et al.*, "Characterization of the neutron induced single event upset in SRAM around high megavoltage clinical accelerators," in *12th European Conference on Radiation and its Effects on Components and Systems–RADECS, Seville* (IEEE, Curran Associates Inc., Red Hook, NY, 2011), pp. 922–925.
[15]NRC, *Health Risks from Exposure to Low Levels of Ionizing Radiation: BEIR VII—Phase 2* (National Academies, Washington, DC, 2006).
[16]D. Bartkowiak *et al.*, "Second cancer after radiotherapy, 1981–2007," Radiother. Oncol. **105**, 122–126 (2012).
[17]A. Berrington de Gonzalez *et al.*, "Proportion of second cancers attributable to radiotherapy treatment in adults: A cohort study in the US SEER cancer registries," Lancet Oncol. **12**, 353–360 (2011).
[18]B. Bednarz, B. Athar, and X. G. Xu, "A comparative study on the risk of second primary cancers in out-of-field organs associated with radiotherapy of localized prostate carcinoma using Monte Carlo-based accelerator and patient models," Med. Phys. **37**, 1987–1994 (2010).
[19]S. Miljanić *et al.*, "Peripheral doses in children undergoing Gamma Knife radiosurgery and second cancer risk," Radiat. Meas. **55**, 38–42 (2013).
[20]L. Irazola *et al.*, "A new online detector for estimation of peripheral neutron equivalent dose in organ," Med. Phys. **41**, 112105 (5pp.) (2014).
[21]B. Sánchez-Nieto *et al.*, "TCP and NTCP: Is that all?," Med. Phys. **39**, 3812 (2012).